





PAPER • OPEN ACCESS

An experimental platform for levitated mechanics in space

To cite this article: Jack Homans et al 2025 Quantum Sci. Technol. 10 035053

View the article online for updates and enhancements.

You may also like

- Adaptive-depth randomized measurement for fermionic observables
 Kaiming Bian and Bujiao Wu
- Multi-mode global driving of trapped ions for quantum circuit synthesis
 Philip Richerme
- <u>Large amplitude mechanical coherent</u> states and detection of weak nonlinearities in <u>cavity optomechanics</u> Wenlin Li, Paolo Piergentili, Francesco Marzioni et al.



Quantum Science and Technology



OPEN ACCESS

RECEIVED

12 March 2025

REVISED

4 June 2025

ACCEPTED FOR PUBLICATION 19 June 2025

PUBLISHED

3 July 2025

Original Content from this work may be used under the terms of the Creative Commons Attribution 4.0 licence.

Any further distribution of this work must maintain attribution to the author(s) and the title of the work, journal citation and DOI.



PAPER

An experimental platform for levitated mechanics in space

Jack Homans¹, Elliot Simcox¹, Jakub Wardak¹, Laura da Palma Barbara¹, Tim M Fuchs¹, Rafael Mufato^{1,2}, Florence Concepcion³, Andrei Dragomir³, Christian Vogt⁴, Peter Nisbet-Jones⁵, Christopher Bridges⁶ and Hendrik Ulbricht^{1,*}

- School of Physics and Astronomy, University of Southampton, SO17 1BJ Southampton, United Kingdom
- ² Department of Physics, Pontifical Catholic University of Rio de Janeiro, Rio de Janeiro, Brazil
- ³ Aquark Technologies Limited, SO50 4SR Eastleigh, Hampshire, United Kingdom
- ⁴ BIAS, Bremer Institut für angewandte Strahltechnik, 28359 Bremen, Germany
- Twin Paradox Labs Inc., K1S 23W4 Ottawa, Ontario, Canada
- ⁶ Surrey Space Center, University of Surrey, GU2 7XH Guildford, Surrey, United Kingdom
- * Author to whom any correspondence should be addressed.

E-mail: H.Ulbricht@soton.ac.uk

Keywords: levitated optomechanics, levitated magnetomechanics, matter wave interferometry, Dark Matter, accelerometry

Abstract

Conducting experiments in extreme conditions has long been the aim of the levitated mechanics field, as it allows for the investigation of new fundamental physics phenomena. Sending these experiments into the micro-g environment of space has been one such milestone, with multiple proposals calling for such a platform. At the same time, levitated sensors have demonstrated a high sensitivity to external stimuli, such as electric, magnetic and gravitational forces, which will only improve in low-vibrational conditions. This paper describes the development of a technology demonstrator for optical and magnetic trapping experiments in space. Our payload represents the first concrete step towards future missions with aims of probing fundamental physical questions: matter-wave interferometry of nanoparticles to probe the limits of macroscopic quantum mechanics, detection of Dark Matter candidates and gravitational waves to test physics beyond the Standard Model, and accelerometry for Earth-observation.

1. Introduction

Levitated optomechanical systems and sensors have been the subject of rapid development and discovery as a quantum technology in recent years, with advances being made into both the research of fundamental phenomena and practical applications. A recent comprehensive review by Gonzalez-Ballestero et al [1] outlines the working principles employed. Levitated mechanical systems are being tailored for research in different fields, such as exploring the limits of quantum mechanics [2, 3], researching the interplay between quantum mechanics and gravity [4], probing physics beyond the standard model of particle physics and cosmology such as for detection of Dark Matter and Dark Energy candidates [5–9], gravitational waves [10, 11] and force sensing [12–15]. The experiments focussed on creating macroscopic quantum states have already identified and worked towards mitigating various decoherence sources such as gas collisions and emission of thermal radiation. However, while terrestrial experiments are capable of strongly isolating test systems from the environment by minimising thermal and mechanical coupling to achieve mechanical quality factors of up to 10^{10} [16], the viability of completely decoupling them from the Earth's seismic and acoustic vibrations is low. Additionally, the effects of gravity on these systems are non-negligible, especially when matter-wave interferometry is considered where limited free-evolution times and possibly gravitational decoherence hinder advances in research. The next big step is therefore to conduct drag-free experiments with levitated systems off-world, as described in a recent vision paper [17].

Dedicated proposals and case studies for nanoparticle interferometry in space have been developed to make a case for testing macroscopic quantum superpositions in space [18], some as part of the general push for quantum technologies in and for space [19–21]. The first consistent proposal for a space-based levitated optomechanical experiment was made in 2012 in the Macroscopic Quantum Resonators (MAQRO) proposal

[22] and has since been updated in 2015 [23] and 2023 [24] for a dedicated satellite mission at Lagrange point L2. The proposal had a close-up assessment by the European Space Agency (ESA) as part of the concurrent design facility (CDF) study under the name of quantum physics platform (QPPF) in 2018.

These proposals detail long-term plans for a dedicated deep-space mission to conduct matter-wave interferometry experiments that would explore the high-mass limits of quantum physics. The platform would also enable research into understanding various decoherence mechanisms, including gravitational decoherence [25]. Alongside providing isolation from low-frequency vibrational noise, conducting these experiments in space will provide the following benefits:

- Longer coherence and free evolution times are required for observing the quantum properties of a released nanoparticle's spatial evolution. The trapping laser's interaction with the nanoparticle acts as a measurement, causing wave-function collapse such that nanoparticles must be released from the trap to allow them to freely evolve. As the required free evolution time for larger nanoparticles ranges between 100 ms to 100 s [26], terrestrial experiments cannot conduct these tests as gravity would accelerate the particles out of the trapping region during this period. In space, this issue is removed, such that experiments are limited solely by the control of the nanoparticle's initial thermal motion [27].
- Increased distance from large gravitational fields whose time dilation affects could cause dephasing between different superposition branches [28, 29].
- Exposure to a subset of Dark Matter/exotic matter candidates that would otherwise be shielded by the Earth's atmosphere [30, 31]. Signals from some interstellar Dark Matter candidates such as anisotropic Dark Matter 'wind' may give a directional signal that would be measurable by the levitated test masses.

In the context of sensing, force and acceleration sensing using freely falling test masses has a proud history in space under the GRACE [32], GOCE [33] and LISA Pathfinder missions where satellite-based accelerometers were used for gravimetry with the purpose of satellite geodesy and gravity mapping. LISA Pathfinder delivered one of the most sensitive accelerometers to date [34]. Levitation-based sensors such as those used in our payload hold promise to deliver sensitive accelerometers operating in the quantum domain at comparably large-mass and benefitting from highly spatially resolved position detection based on quantum optomechanics [35].

Here we describe the realisation and testing of a payload to undertake levitated mechanical experiments in space. Through a successful application into the 'ESA Payload Masters' competition, a position has been secured with The Exploration Company for our experiment to be launched into low Earth orbit in June 2025 for a 3 hour flight to experience approximately 30 minutes of micro-g conditions as part of their 'Mission Possible' Nyx flight. The payload has been constructed in collaboration with Twin Paradox Labs, Surrey Space Centre, ZARM, BIAS and Aquark Technologies such that both optical and magnetic traps can be created in a compact volume and the experiments run autonomously, on low power, and without telemetry. We shall discuss the theory underlying the two levitation experiments, the mechanical, optical and electrical design of the payload, the environmental testing it has undergone, and present preliminary data that has been collected from it prior to launch.

2. Brief physics of trapping

While optical [36] and magnetic [37] levitation rely on very different fundamental phenomena, calculating their levitation dynamics is surprisingly similar, so shall be discussed in parallel. Optical and magnetic traps rely respectively on the polarizability α of the silica nanoparticle and effective magnetization **M** of the diamagnetic graphite sheet being trapped. These properties are defined as:

$$\alpha = 4\pi n^2 \varepsilon_0 r^3 \frac{m^2 - 1}{m^2 + 2},\tag{1}$$

$$\alpha = 4\pi n^2 \varepsilon_0 r^3 \frac{m^2 - 1}{m^2 + 2},$$

$$\mathbf{M} = \frac{1}{\mu_0} \chi \cdot \mathbf{B}.$$
(1)

In equation (1), n is the nanoparticle's refractive index, ε_0 the vacuum permittivity, r the nanoparticle's radius and $m = n/n_m$ the relative refractive index where n_m is the surrounding medium's refractive index. In equation (2), χ is the material's magnetic susceptibility tensor, which, in the graphite's body frame, is equal to the tensor's diagonal ($\chi = \text{diag}(\chi_x, \chi_y, \chi_z)$), μ_0 is vacuum permeability, and **B** is the external trapping magnetic field.

 α and **M** can be used to calculate the trapping forces applied to the nanoparticle and graphite sheet as the optical gradient force \mathbf{F}_{grad} and the magnetic force density $\mathbf{f}(\mathbf{r}) = (\mathbf{M} \cdot \nabla) \mathbf{B}$ acting on the graphite.

$$\mathbf{F}_{\text{grad}} = \frac{4\pi \, nr^3}{c} \left(\frac{m^2 - 1}{m^2 + 2} \right) \nabla I(\mathbf{r}_{\text{rad}}, \mathbf{z}), \tag{3}$$

$$\mathbf{f}(\mathbf{r}) = \frac{1}{2\mu_0} \nabla \left(\chi_x B_x^2 + \chi_y B_y^2 + \chi_z B_z^2 \right). \tag{4}$$

In equation (3), c is the speed of light in a vacuum and $I(\mathbf{r}_{rad}, \mathbf{z})$ is the trapping laser beam's Gaussian intensity profile. In equation (4), we have chosen z to be the graphite's normal (vertical) plane (see figure 1), such that $\chi_z \gg \chi_{x,y}$. The expanded calculations required to transform $\mathbf{f}(\mathbf{r})$ into the magnetic force $\mathbf{F}_{mag}(\mathbf{r})$ acting on the graphite above a single magnet array can be seen in [37, 38], and adapting them for our trap would be trivial.

Using these equations, we can calculate the position \mathbf{r} dependent optical (equation (5)) and magnetic (equation (6)) spring stiffnesses k for each axis i of each trap:

$$k_{(x,y)} = \frac{4\alpha (\mathrm{NA})^4 \pi^3}{c\varepsilon_0 \lambda^4} P_0, \qquad k_z = \frac{2\alpha (\mathrm{NA})^6 \pi^3}{c\varepsilon_0 \lambda^4} P_0, \tag{5}$$

$$\mathbf{k}(\mathbf{r}) = -\nabla \mathbf{F}_{\text{mag}}(\mathbf{r}). \tag{6}$$

In equation (5), NA is the numerical aperture of the parabolic mirror that focuses the laser beam to create the optical trapping region, λ the trapping laser's wavelength, and P_0 the trapping laser power.

Using the values of k and the masses m of the levitated oscillators, the oscillation frequencies can be predicted for each trap using $\omega_i = \sqrt{\frac{k_i}{m}}$.

3. Payload trap designs

3.1. Optical trap

The single-beam optical trap uses a high NA (NA \sim 0.9) aluminium parabolic mirror (*Wielandts UMPT*), to focus a \sim 79 mW 1555 nm laser beam, collimated by an output coupler (*Thorlabs PAF2A-18 C*), to create the trapping region. Details of the parabola trap can be found in previous works [36, 39]. A roughened aluminium iris was placed in front of the parabolic mirror to block back-reflections from the mirror's flat mirrored face. The trap is designed to capture ϕ 300 nm silica nanoparticles (*Bang Laboratories SSD2001*) ejected from a 3.12 \times 13.22 \times 1.05 mm (\pm 0.01 mm) PTFE-coated glass cantilever positioned 11 \pm 1 mm from the trap centre that will be excited by a piezoelectric actuator (*Piezo Drive SA030310*). The viewport used to provide optical access was anti-reflection coated for 1555 nm (*Torr Scientific Ltd*) to prevent back-reflections off the viewport from obscuring the nanoparticle's signal.

3.2. Magnetic trap

The passive magnetic trap levitates a pyrolytic graphite flake (K & J Magnetics Ltd PG3) between two 2×2 Halbach arrays of $5 \times 5 \times 2$ mm samarium cobalt magnets (SMMagnetics Sm2Co17-32) [37, 40]. In terrestrial experiments, the graphite is held by gravity above a single repelling magnet array. In our setup, the second array will replace gravity and, in micro-g conditions, the graphite shall levitate around the midpoint between the arrays. The arrays are arranged in an attracting configuration as this produces a more stable trapping potential. The viability of this setup has been demonstrated in the temporary micro-g conditions of the ZARM drop-tower.

The graphite's position is measured using a shadow-detection method, where a ~ 10 mW $\phi 1.42$ mm 1555 nm laser beam is shone horizontally from a output coupler (*Thorlabs PAF2-A7C*) past the graphite to a large surface area photodetector (*Thorlabs FDG05*), with the laser beam offset from the trap's midpoint to maximize sensitivity. Changes in the graphite's position will therefore proportionally modulate the detected laser power. The trap's configuration (shown in figure 1) provides the greatest sensitivity to the graphite's *z*-displacement, but the graphite's surface roughness and slight misalignment from the horizontal enables detection of its x and y motion.

The graphite was laser cut into a $4.94 \times 4.95 \times 0.66 \ (\pm 0.01)$ mm square and patterned into a fish-bone configuration (*Laser Micromachining Ltd*). The patterning (shown in figure 1) splits the eddy-currents

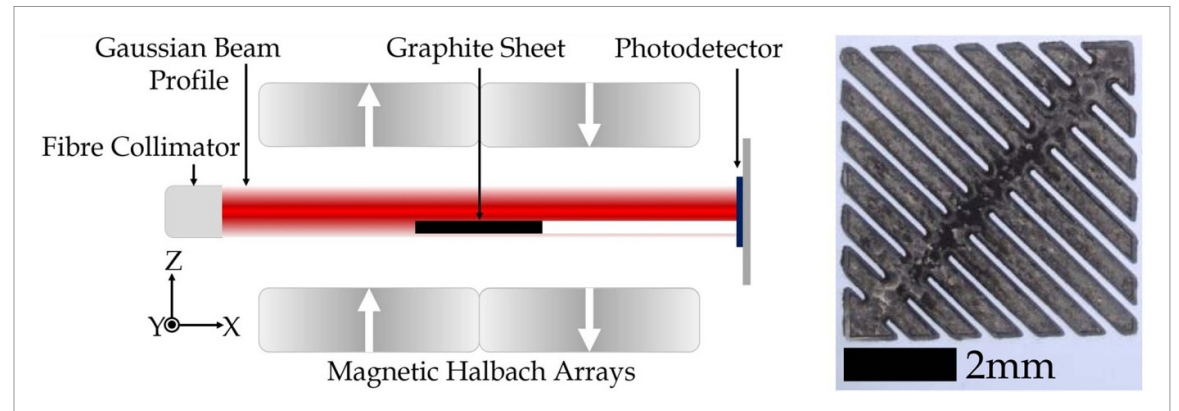


Figure 1. Magnetic trap layout with optical detection. Left: An illustration of the dual Halbach array passive magnetic trap with the laser beam offset from the trap's centre. Graphite levitation position is indicated by the black rectangle in the centre. Laser light is blocked by the graphite and detected in transmission on a photodetector. Right: A photograph of pyrolytic graphite sheet laser cut into a fish-bone configuration.

induced by the graphite's motion relative to the magnets into smaller loops, reducing the forces generated that oppose the graphite's motion and enhancing the Q-factor. The graphite was coated in a thin layer of vacuum compatible epoxy (Epotek~302-3~M) to increase its strength and durability, and to increase the graphite's mass from $26.2\pm0.2~mg$ to $28.0\pm0.2~mg$, which therefore increased its acceleration sensitivity.

3.3. Vacuum chamber

The two traps were placed inside a custom two-chambered CF16 vacuum chamber machined from austenitic stainless steel (shown in figure 2). The traps were placed in separate chambers to accommodate the different vacuum pressure requirements of each trap. 0.1 mbar was chosen for the optical trap to maintain enough gas damping to aid with loading nanoparticles. 10^{-3} mbar was chosen for the magnetic trap as eddy-current damping was found to dominate gas damping below this pressure, and time constraints prevented further pumping. The optical trap's chamber had 4 ports, allowing for optical access, electrical feedthrough, piezo positioning and vacuum pumping. The magnetic trap's chamber had 3 ports; two for optical access and one for vacuum pumping.

Active vacuum pumping and venting to space is not available during the mission, so a non-evaporable getter was coated onto the chambers' internal surfaces (*Aquark Technologies*). This will maintain the chambers' pressures for the 6 month period between payload completion and the mission launch, and throughout the mission. Once the chambers had been evacuated, they were baked-out, both to improve the vacuum and to activate the getter, and then pinched off. Additionally, sapphire viewports (*Lewvac SVP-UV-11.6-16CF*) were used to provide optical access into the chambers, as they are more effective at preventing light gases from leaking into the chambers compared to standard borosilicate viewports.

4. Payload design

Various parameters were set by The Exploration Company for the design and configuration of the payload (shown in table 1).

The payload's weight-dependent power allowance resulted in it being designed to weigh 10 kg to obtain the full 10 W_{av} power allowance. This meant that, unconventionally, large parts of the payload were made from solid steel and aluminium. If the payload could be exposed to the vacuum of space instead of needing a vacuum chamber and the power-per-weight requirement was removed, the payload's mass could be reduced to \sim 1 kg.

One of the payload's end-plates was designed as a heat sink for the laser driver PCB and FPGA (see section 5), while the other was recessed to hold the optical trap's photodetector (see section 6). Both end-plates were bolted to the stainless steel baseplate which was designed with M10 through-holes for bolting the payload to the Nyx capsule. The end-plates were also held together at the top of the payload by aluminium stringers, while larger stringers between the two end-plates held the vacuum chamber near the payload's midpoint. Another stringer was added between the top stringers to hold the optical fibre mating sleeves. Stainless steel cover-plates were attached to the stringers and end-plates to enclose the payload. Images of the completed payload can be seen in figure 3. To ensure that all structural components would be secure throughout the mission, all threaded parts used locking threads (*Spiralock*) and a threadlocking agent

Table 1. The technical specifications set by The Exploration Company for the payload design.

Specification
$20 \times 20 \times 15 \mathrm{cm}$
≤10 kg
$1 \text{W}_{\text{av}}/\text{kg} \leqslant 10 \text{W}_{\text{av}}, 84 \text{W}_{\text{peak}}, 28 \text{V}$
1 GB main storage, 100 MB backup
0→50°C

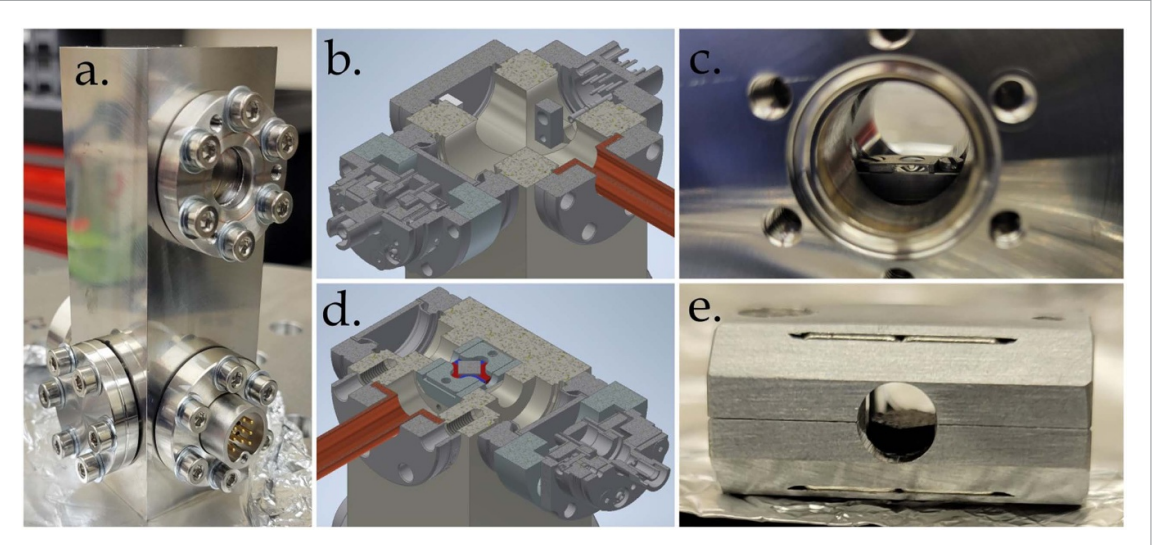


Figure 2. Details of vacuum chamber with optical and magnetic traps. (a) The custom CF16 vacuum chamber used in the payload. (b) A CAD model of the optical trap vacuum chamber, showing the parabolic mirror bolted to the vacuum chamber, opposing the laser collimator. The electrical feedthrough, piezoelectric actuator and copper pinch-off tube are also shown. (c) The iris stuck over the top of the parabolic mirror. (d) A CAD model of the vacuum chamber used for magnetic trapping. The graphite and one magnet array are shown in their holder, along with the two viewports and the copper pinch-off tube. (e) A prototype of the magnetic trap, with the magnets held 4 mm apart and the fish-bone pattern, epoxy coated graphite sheet levitating between the two arrays.

(*Loctite 242*). Similarly, all internal wires and optical fibres were secured with dots of epoxy (*3 M DP190*) at least every 2 cm.

5. Electronics

The laser (*Thorlabs DFB1550P*) used in the experiments is driven by a custom laser driver PCB, produced by a joint team from Twin Paradox Labs and Surrey Space Centre [41, 42], that was controlled by an FPGA (*Xilinx Artix 7 A200*). The laser driver enables measurement and control of the laser's output and thermo-electric controller, and also has capabilities for analogue input and output, PID control and 16-bit data saving. The laser driver and FPGA jointly draws approximately 7 W.

The 28 V_{DC} supply from the Nyx capsule is passed through a fifth-order low pass filter to protect both the Nyx capsulse and the payload from voltage fluctuations. The input is then internally converted to a 5 V_{DC} line and $\pm 12\,V_{DC}$ rails. The $\pm 12\,V_{DC}$ is used to power the optical trap's photodetector (*Thorlabs PDBEVAL1*) while the 5 V_{DC} powers the remaining systems, namely the laser driver PCB and attached FPGA, the optical trap's piezo kicking system and a microcontroller (*Arduino Portenta H7*) used to control internal signals and acquire experimental data. The 5 V_{DC} also provides a reverse bias to the magnetic trap's photodetector (*Thorlabs FDG05*) to increase the detector's sensitivity.

The microcontroller has 3 internal analogue-digital converters which are used to collect data from the two photodetectors and a reference accelerometer ($Analogue\ Devices\ EVAL\text{-}ADXL354BZ$). The data will be collected with 16-bit resolution in 8 MB packets (limited by the microcontroller's RAM) and saved with duplicates on an internal micro-SD card to protect the data from corruption. Before reaching the microcontroller, the photodetectors' signals are passed through band-pass filters, DC-shifted and amplified to maximize the system's sensitivity. The data from the optical and magnetic traps is acquired, respectively, at sampling rates of 500 kSa s⁻¹ and 10 kSa s⁻¹ to allow for sufficient bandwidth to measure the predicted oscillation frequencies of each trap. The accelerometer data is only saved alongside the magnetic trap data, as the nanoparticle is too light to effectively measure the same vibrational noise floor.

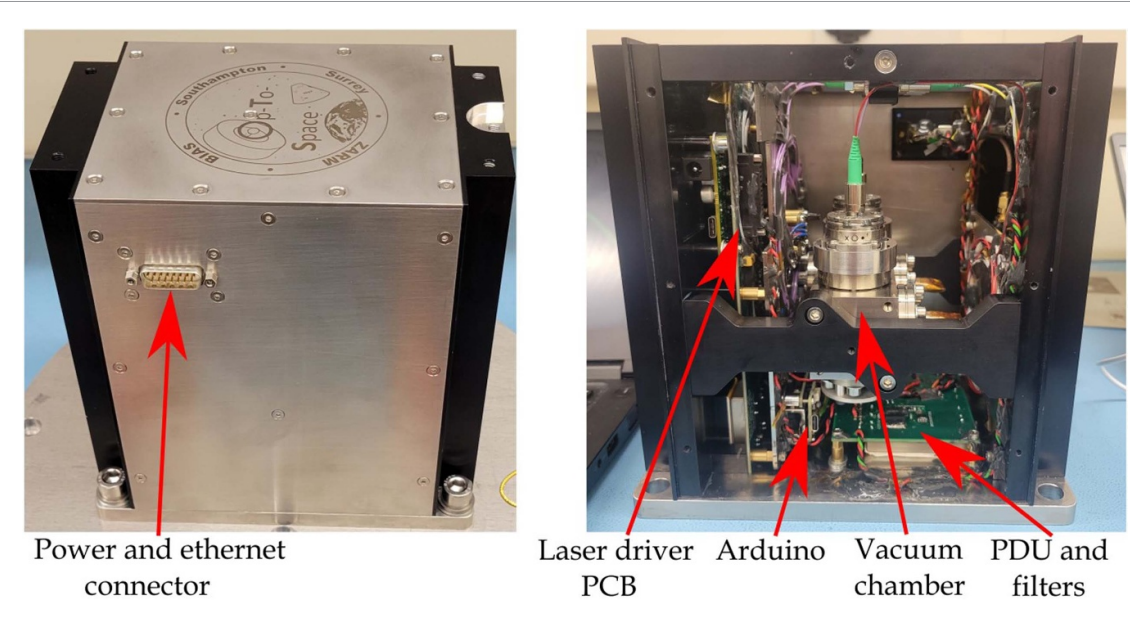


Figure 3. Photographs of the flight model of payload for levitated mechanical experiments in space. Left: The external form of the payload. Right: The internal layout of experimental components in the payload. The system operates fully autonomously and starts experimental protocols after a trigger from the spacecraft.

6. Optics system and laser

A system of optical fibres pass the trapping/monitoring laser around the payload. A 90:10 beam-splitter (*Thorlabs TN1550R2A1*) couples the beam from the laser's output (*Thorlabs DFB1550P*, 100 mW CW at 1555 nm) into the traps, sending 90% to the optical trap and 10% to the magnetic trap. The optical trap's beam is then passed through a circulator (*Thorlabs 6015-3-APC*) which circulates the incident light to the optical trap, and couples the returning light into one arm of a balanced photodetector (*Thorlabs PDBEVAL1 with PDB770C*).

7. Proof of functionality

An identical optical trap was used to trap a ϕ 300 nm silica nanoparticle. The trap was loaded using a medical nebuliser. Figure 4 shows a power-spectral density (PSD) recovered from the light returning from the trap. The oscillation frequencies observed match well with the expected range of 10–100 kHz. The piezo system that will be used to load nanoparticles into the trap during autonomous operation was tested in various configurations, and it was shown that, as long as gravity did not excessively oppose the nanoparticle's trajectory, the nanoparticles could be ejected towards the trap. Time-of-flight measurements indicated initial ejection speeds of 10–20 cm s⁻¹, in-line with previous work [43]. However, to date, we have yet to capture nanoparticles launched using this method. It is believed that the ejected nanoparticles are accelerated by gravity to such a degree that the trap cannot slow them sufficiently. We therefore predict that, in micro-g conditions, the nanoparticles will travel slower towards the trap and the gas damping provided by the 0.1 mbar vacuum will sufficiently slow the nanoparticles such that they can be captured by the conservative trapping potential.

While the payload was undergoing software testing (see section 8), data was taken with the magnetic trap in the payload using all the systems that will be used throughout the mission. The PSD of the graphite's motion (shown in figure 4) shows that the graphite's multiple distinct oscillation frequencies can be detected and match well with the predicted frequency range of 1–100 Hz.

In terrestrial experiments, gravity shifts the graphite away from the magnetic trap's centre to a new equilibrium position with different trap spring constants. When in micro-g conditions, we expect the graphite to instead oscillate around the trap's centre, resulting in a 19% decrease in its z-oscillation frequency compared to the data shown in figure 4. While the optically levitated nanoparticle is also shifted away from its trap centre in terrestrial experiments, it has been shown that the change in oscillation frequency in micro-g is not experimentally measurable [44].

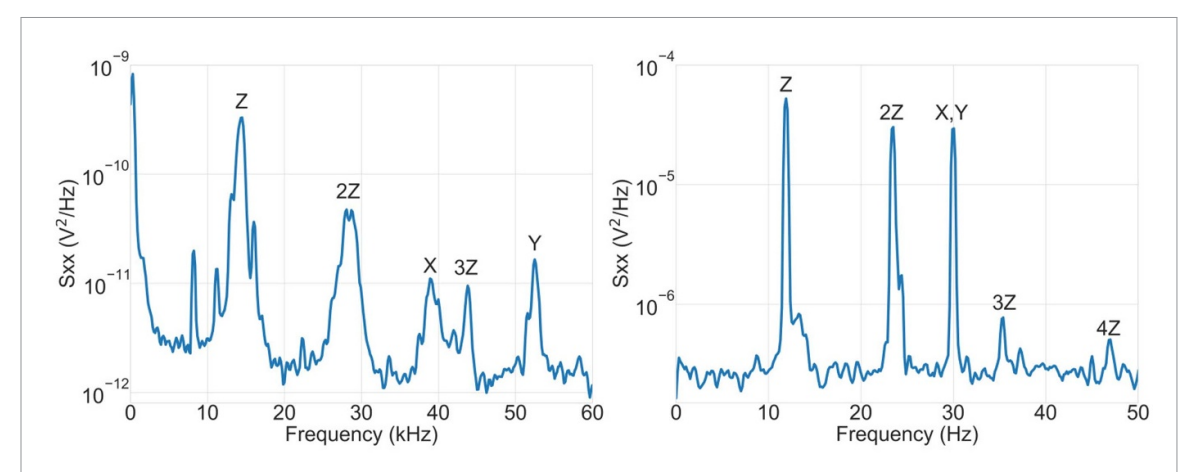


Figure 4. Demonstration of traps and detection of motion. Power spectral densities (PSDs) of time traces taken for both traps without active stabilisation and by optical detection [45]. Observed motional frequencies are in good agreement with theoretically modelled ones. Left: The spectrum taken using an identical optical trap and vacuum chamber. A 70 mW trapping laser was used to trap a ϕ 300 nm silica nanoparticle in 0.46 mbar after it had been loaded into the trap with a nebuliser. The PSD shows translational x, y, z-motional degrees and coupling. Right: The PSD of the data taken during the software testing using the magnetic trap in the flight model (FM) payload at \sim 10⁻³mbar. The peaks in the graph represent the graphite's x, y, z-translational modes and coupling.

8. Environmental testing

To ensure that the payload will operate safely and completely throughout its mission, it has been subjected to multiple rounds of testing. Two versions of the payload were constructed, an engineering model (EM) and a flight model (FM). Electromagnetic (EMC) and thermal testing was conducted on the EM, along with the first round of mechanical testing. The payload's design was then modified based on the testing results before the FM was constructed. The FM then underwent the second round of mechanical testing, power characterization testing and software tests to ensure it met The Exploration Company's launcher requirements.

Thermal testing assessed the payload's responses to changing external thermal environments. The test was conducted at Surrey Space Centre using their Kambie Climatic Chamber (KK-190 CHULT). The payload's functionality was assessed in steps between 0° C and 40° C, and the payload was then subjected to thermal stress testing, varying its temperature between -40° C and $+70^{\circ}$ C in seven cycles over 5 days. No effects were observed and the payload retained full functionality.

The EM underwent three mechanical testing phases. Characterization of mechanical properties involved determining its mass and centre of gravity. Vibrational testing involved conducting resonance searches before and after random vibration tests to determine the payload's fundamental modes and ensure that it will not be adversely affected by the mission's vibrational conditions. Shock testing ensured that the mission's shock environment will not affect the payload's functionality. The FM also had its mechanical properties characterized and underwent acceptance level vibrational tests to assess its build quality and confirm that it was within design tolerances. The EM's vibrational and shock tests and FM's vibrational tests were conducted using Surrey Space Centre's mechanical testing facilities. An LDS Model V826 shaker head was used to conduct the vibrational tests in all three of the payload's axes, while a custom shock testing table was used to exert sufficient forces on the EM in each axis. Modifications were made to the payload's design following testing on the EM such that the FM passed all mechanical testing stages.

EMC testing of the EM was conducted at the BAE Systems Rochester testing facility, and consisted of 4 parts; conducted emission, conducted susceptibility, radiated emission and radiated susceptibility. The testing levels for each of these can be seen in table 2. The conducted emission and susceptibility tests were passed without issue. Spikes in the payload's emission were detected during the radiated emission test, but were agreed to be acceptable by The Exploration Company. The payload was affected by the radiated susceptibility test, but the affected electronic component was identified and replaced with a compatible alternative for the FM.

Software testing checked that the payload could interact with the Nyx capsule throughout the mission. The payload was tested in its various operational modes and its response to all possible input signals was assessed. Additionally, the payload's data output was inspected following the test to ensure that all data was collected (see figure 4). The test showed full functionality under all requirements.

Table 2. The testing levels for each of the EMC testing phases, listed where applicable with their spectral range [46].

Test	Requirements
Conducted Emission	[30;10k] Hz: MIL-STD-461 CE101-4: Curve 2 '28 VOLTS OR BELOW' [10k;10 M] Hz: MIL-STD-461 CE102-1: Basic curve '28 V'
Conducted Susceptibility	[30;150k] Hz: MIL-STD-461 CS101-1: Curve 2 '28 VOLTS OR BELOW' [10k;200 M] Hz: MIL-STD-461 CS114-1: Curve 3 'SPACE'
Radiated Emission Radiated Susceptibility	Custom requirements from The Exploration Company. Custom requirements from The Exploration Company.

The power characterization test assessed the payload's power usage throughout the mission—specifically the initial current in-rush when switched on, the change in power consumption when the experimental sequence started and terminated, and the power drain when the payload was switched off. Additionally, the payload's thermal output was measured at multiple locations to ensure the Nyx capsule and surrounding payloads would not be affected by the payload. The test showed that the current in-rush was below the required latching current limit and that the average power consumption was 10.94 W—within 10% of the expected 10 W.

9. Conclusion and outlook

We have described the design and realisation of a space payload for in-orbit levitated mechanical experiments that will be launched in June 2025. The payload contains two types of trap, one optical and one magnetic, which may assist in optimizing success of our first space mission. The experiments aim to demonstrate autonomous dry loading of nanoparticles into an optical trap in micro-g conditions, as well as quantifying the acceleration sensitivity and noise floor attainable with a passive magnetic trap in such conditions. The payload has passed all tests to specifications for space qualification and has demonstrated full functionality of detection of mechanical modes in both traps.

Our payload has been designed as a prototype to build on for future missions, with many of the internal systems already capable of more functionality than are currently being used. It is hoped that, in future missions, we will be able to parametrically feedback cool the optically levitated nanoparticle's centre-of-mass motion such that we can increase the spatial coherence in the motional state ready for conducting matter-wave interferometry experiments, as well as reducing the influences of other decoherence sources such that we can produce interference patterns with high visibility. Additionally, further missions are in development that aim to use the passive magnetic traps to detect certain Dark Matter candidates.

Data availability statement

The data that support the findings of this study are openly available at the following URL/DOI: https://doi.org/10.5258/SOTON/D3411.

Acknowledgments

We thank James Chalk, Philip Connell, Mark Bampton, Damon Grimsey, Jamie Faux, Oliver Warner, Leigh Allen, Luca Ferrain, Colin Chau, and Robin Elliott for their expert technical support and consultation. We also thank the Space South Central cluster for their support. HU would like to thank the EU COST action QTSpace and in particular Angelo Bassi, Mauro Paternostro, Matteo Carlesso, Alessio Belenchia, Giulio Gasbarri and Rainer Kaltenbaek for pushing large-mass quantum experiments in space and the MAQRO proposal. This project has been made possible by the ESA Payload Master's competition, providing us with a place in The Exploration Company's 'Mission Possible' launch. JH, ES, JW, LB, TF, and HU acknowledges funding by the EU EIC Pathfinder project QuCoM (101046973). We thank for support the UKRI EPSRC (EP/W007444/1, EP/V000624/1 and EP/X009491/1), the Leverhulme Trust (RPG-2022-57) and the QuantERA II Programme (project LEMAQUME) that has received funding from the European Union's Horizon 2020 research and innovation programme project QuCoM under Grant Agreement No 101017733. CV acknowledges support from DLR project NaiS (50WM2180).

References

- Gonzalez-Ballestero C, Aspelmeyer M, Novotny L, Quidant R and Romero-Isart O 2021 Levitodynamics: levitation and control of microscopic objects in vacuum Science 374 eabg3027
- [2] Millen J and Stickler B A 2020 Quantum experiments with microscale particles Contemp. Phys. 61 155-68
- [3] Carlesso M, Donadi S, Ferialdi L, Paternostro M, Ulbricht H and Bassi A 2022 Present status and future challenges of non-interferometric tests of collapse models Nat. Phys. 18 243–50
- [4] Bose S, Fuentes I, Geraci A A, Khan S M, Qvarfort S, Rademacher M, Rashid M, Toroš M, Ulbricht H and Wanjura C C 2025 Massive quantum systems as interfaces of quantum mechanics and gravity Rev. Mod. Phys. 97 015003
- [5] Moore D C and Geraci A A 2021 Searching for new physics using optically levitated sensors Quantum Sci. Technol. 6 014008
- [6] Kilian E et al 2024 Dark matter searches with levitated sensors (arXiv:2401.17990)
- [7] Amaral D W, Uitenbroek D G, Oosterkamp T H and Tunnell C D 2024 First search for ultralight dark matter using a magnetically levitated particle (arXiv:2409.03814)
- [8] Kalia S, Budker D, Kimball D F J, Ji W, Liu Z, Sushkov A O, Timberlake C, Ulbricht H, Vinante A and Wang T 2024 Ultralight dark matter detection with levitated ferromagnets Phys. Rev. D 110 115029
- [9] Adelberger E et al 2022 Snowmass white paper: precision studies of spacetime symmetries and gravitational physics (arXiv:2203.09691)
- [10] Arvanitaki A and Geraci A A 2013 Detecting high-frequency gravitational waves with optically levitated sensors Phys. Rev. Lett. 110 071105
- [11] Pontin A, Mourounas L S, Geraci A A and Barker P F 2018 Levitated optomechanics with a fiber fabry–perot interferometer New J. Phys. 20 023017
- [12] Ranjit G, Atherton D P, Stutz J H, Cunningham M and Geraci A A 2015 Attonewton force detection using microspheres in a dual-beam optical trap in high vacuum *Phys. Rev. A* 91 051805(R)
- [13] Hempston D, Vovrosh J, Toroš M, Winstone G, Rashid M and Ulbricht H 2017 Force sensing with an optically levitated charged nanoparticle Appl. Phys. Lett. 111 133111
- [14] Monteiro F, Li W, Afek G, Li C-l, Mossman M and Moore D C 2020 Force and acceleration sensing with optically levitated nanogram masses at microkelvin temperatures *Phys. Rev. A* 101 053835
- [15] Fuchs T M, Uitenbroek D G, Plugge J, van Halteren N, van Soest J-P, Vinante A, Ulbricht H and Oosterkamp T H 2024 Measuring gravity with milligram levitated masses Sci. Adv. 10 eadk2949
- [16] Dania L, Bykov D S, Goschin F, Teller M, Kassid A and Northup T E 2024 Ultrahigh quality factor of a levitated nanomechanical oscillator Phys. Rev. Lett. 132 133602
- [17] Belenchia A, Carlesso M, Donadi S, Gasbarri G, Ulbricht H, Bassi A and Paternostro M 2021 Test quantum mechanics in space-invest us 1 billion Nature 596 32–34
- [18] Gasbarri G, Belenchia A, Carlesso M, Donadi S, Bassi A, Kaltenbaek R, Paternostro M and Ulbricht H 2021 Testing the foundation of quantum physics in space via interferometric and non-interferometric experiments with mesoscopic nanoparticles Commun. Phys. 4 155
- [19] Belenchia A et al 2022 Quantum physics in space Phys. Rep. 951 1–70
- [20] Kaltenbaek R et al 2021 Quantum technologies in space Exp. Astron. 51 1677–94
- [21] Bassi A et al 2022 A way forward for fundamental physics in space npj Microgravity 8 49
- [22] Kaltenbaek R, Hechenblaikner G, Kiesel N, Romero-Isart O, Schwab K C, Johann U and Aspelmeyer M 2012 Macroscopic quantum resonators (MAQRO) testing quantum and gravitational physics with massive mechanical resonators *Exp. Astron.* 34 123–64
- [23] Kaltenbaek R et al 2016 Macroscopic quantum resonators (MAQRO): 2015 update EPJ Quantum Technol. 3 1–47
- [24] Kaltenbaek R et al 2023 Research campaign: macroscopic quantum resonators (MAQRO) Quantum Sci. Technol. 8 014006
- [25] Bassi A, Großardt A and Ulbricht H 2017 Gravitational decoherence Class. Quantum Grav. 34 193002
- [26] Wardak J, Georgescu T, Gasbarri G, Belenchia A and Ulbricht H 2024 Nanoparticle interferometer by throw and catch Atoms 12 7
- [27] Bateman J, Nimmrichter S, Hornberger K and Ulbricht H 2014 Near-field interferometry of a free-falling nanoparticle from a point-like source Nat. Commun. 5 4788
- [28] Pikovski I, Zych M, Costa F and Brukner Č 2015 Universal decoherence due to gravitational time dilation Nat. Phys. 11 668-72
- [29] Zych M 2017 Quantum Systems Under Gravitational Time Dilation (Springer)
- [30] Bateman J, McHardy I, Merle A, Morris T R and Ulbricht H 2015 On the existence of low-mass dark matter and its direct detection *Sci. Rep.* 5 8058
- [31] Riedel C J and Yavin I 2017 Decoherence as a way to measure extremely soft collisions with dark matter Phys. Rev. D 96 023007
- [32] Li B et al 2019 Global grace data assimilation for groundwater and drought monitoring: advances and challenges Water Resour. Res. 55.7564–86
- [33] van der Meijde M, Pail R, Bingham R and Floberghagen R 2015 Goce data, models and applications: a review *Int. J. Appl. Earth Obs. Geoinf.* 35 4–15
- [34] Armano M et al 2019 Lisa pathfinder performance confirmed in an open-loop configuration: results from the free-fall actuation mode *Phys. Rev. Lett.* 123 111101
- [35] Aspelmeyer M, Kippenberg T J and Marquardt F 2014 Cavity optomechanics Rev. Mod. Phys. 86 1391-452
- [36] Vovrosh J A 2018 Parametric feedback cooling and squeezing of optically levitated particles PhD thesis University of Southampton
- [37] Romagnoli P, Lecamwasam R, Tian S, Downes J and Twamley J 2023 Controlling the motional quality factor of a diamagnetically levitated graphite plate Appl. Phys. Lett. 122 094102
- [38] Tian S, Jadeja K, Kim D, Hodges A, Hermosa G, Cusicanqui C, Lecamwasam R, Downes J and Twamley J 2024 Feedback cooling of an insulating high-Q diamagnetically levitated plate *Appl. Phys. Lett.* 124 124002
- [39] Vovrosh J, Rashid M, Hempston D, Bateman J, Paternostro M and Ulbricht H 2017 Parametric feedback cooling of levitated optomechanics in a parabolic mirror trap *JOSA B* 34 1421–8
- [40] Chen X, Ammu S K, Masania K, Steeneken P G and Alijani F 2022 Diamagnetic composites for high-Q levitating resonators Adv. Sci. 9 2203619
- [41] Chau H, Boyle I, Nisbet-Jones P and Bridges C 2022 Designing avionics for lasers & optoelectronics 4th Symp. on Space Educational Activities (Universitat Politècnica de Catalunya)
- [42] Chau H K, Bridges C and Nisbet-Jones P 2023 Portable frequency stabilized lasers for quantum technologies using digital techniques *IEEE Trans. Instrum. Meas.* 72 1–6

- [43] Khodaee A, Dare K, Johnson A, Delić U and Aspelmeyer M 2022 Dry launching of silica nanoparticles in vacuum *AIP Adv.* 12 125023
- [44] Prakash G, Herrmann S, Bergmann R B and Vogt C 2025 Release and recapture of silica nanoparticles from an optical trap in weightlessness (in preparation)
- [45] Homans J et al 2025 Data for the paper 'An experimental platform for levitated mechanics in space' University of Southampton Institutional Repository (available at: https://eprints.soton.ac.uk/500821/)
- [46] USA Department Of Defense Interface Standard 2015 Requirements for the control of electromagnetic interference characteristics of subsystems and equipment